Journal of Hydraulic and Water Engineering (JHWE), Vol. 3, NO. 1, 67-93

Shahrood University of Technology

Journal of Hydraulic and Water Engineering (JHWE)

Journal homepage: https://jhwe.shahroodut.ac.ir

Iranian Hydraulic Association (IHA)

Assessment of Hydroclimatic Variability Using Observations and MERRA-2 Data for Sustainable Kalamu Dam Management

André Mampuya Nzita [1,2*], Manifeste Wala Kafuti [2], Georges-Noel Tiersmondo Longandjo [3], Raphael Tshimanga Muamba[2],Guyh Dituba Ngoma [4], Clément N'zau Umba-di-Mbudi [1,5]

[1] President Joseph Kasa-Vubu University, Polytechnic Faculty, Boma, Democratic Republic of the Congo
[2] Regional School of Water (ERE), University of Kinshasa (UNIKIN) and Congo Basin Water Resources Research Centre, University of Kinshasa, Kinshasa, Democratic Republic of the Congo
[3] Nansen-Tutu Centre for Environmental Marine Research, Department of Oceanography, University of Cape Town,Rondebosch, South Africa and Hydro-Environmental Research Laboratories, Department of Meteorology, Higher Institute of Applied Techniques, Kinshasa, Democratic Republic of the Congo
[4] University of Quebec in Abitibi-Temiscamingue, School of Engineering, Rouyn-Noranda, Canada
[5] University of Kinshasa, Faculty of science and technology, Kinshasa, Democratic Republic of the Congo

Article Info

Article history:

Received 27 March 2025
Received in revised form 9 February 2026
Accepted 11 June 2026
Published online 14 June 2026

DOI:
10.22044/jhwe.2026.15995.1058

Keywords
Hydroclimatic Variability
Water Balance
MERRA-2 Reanalysis
Reservoir Management
Kalamu Intake Dam

Abstract

Water resources stored in small reservoirs and intake dams are essential for ensuring a reliable water supply, particularly in regions exposed to strong hydroclimatic variability. Climate change and increasing fluctuations in precipitation and evaporation patterns are creating new challenges for the sustainable management of water infrastructures. In Boma, Democratic Republic of the Congo, the Kalamu intake dam experiences recurrent seasonal water shortages due to reduced river discharge during the dry season, reservoir eutrophication, and growing pressure on available water resources. This study aimed to assess the hydroclimatic variability of the Kalamu catchment and evaluate its implications for water availability, reservoir performance, and long-term water resource sustainability. Monthly precipitation and evaporation observations collected at the Boma meteorological station were combined with MERRA-2 reanalysis data covering the period 1992–2023. Statistical analyses, including Pearson correlation, coefficient of determination (R^2), Mean Absolute Error (MAE), Root Mean Square Error (RMSE), and bias, were used to evaluate the agreement between observed and reanalysis datasets. Hydroclimatic variability was investigated through water balance analysis, Z-score classification of hydrological years, and trend detection using the Mann–Kendall test and Sen's slope estimator. The results showed that MERRA-2 satisfactorily reproduced general precipitation patterns but moderately overestimated rainfall and smoothed extreme events. In contrast, evaporation estimates exhibited poor agreement with observations, characterized by a strong negative bias and weak correlation. The hydroclimatic analysis revealed alternating wet and dry years, a cumulative water deficit of 4982.05 m^3, and a required storage capacity of 209.88 m^3 compared with the current reservoir capacity of only 160 m^3. Trend analyses indicated no statistically significant long-term changes in precipitation, evaporation, or water balance, although substantial interannual variability was observed. The study concludes that the Kalamu dam remains vulnerable to seasonal water shortages. Increasing storage capacity, improving reservoir management, strengthening hydroclimatic monitoring, and applying bias correction to reanalysis datasets are recommended to enhance water supply reliability. Furthermore, current hydroclimatic conditions suggest that the installation of a mini-hydropower plant is not presently feasible because water availability remains insufficient to guarantee sustainable energy production without compromising the primary water-supply function of the dam.

1. Introduction

Water resources stored in small reservoirs and intake dams play a critical role in ensuring water supply reliability, particularly in regions characterized by strong hydroclimatic variability. Changes in precipitation, evaporation, and water balance directly influence reservoir performance and water availability. Recent studiaes have shown that climatic variability increasingly affects reservoir storage dynamics worldwide, reducing the capacity of water infrastructures to satisfy growing water demands (Hou et al., 2022). In Africa, fluctuations between wet and dry periods have become a major concern for sustainable water resources management and climate adaptation strategies (Alahacoon et al., 2022; Balme et al., 2006). The Kalamu intake dam, located in Boma, Democratic Republic of the Congo, is particularly vulnerable to seasonal water shortages due to reduced river discharge during the dry season and increasing environmental pressures (Mampuya et al., 2026). Beyond its role in water supply, the dam may also offer opportunities for future renewable energy development through the installation of a mini-hydropower plant. However, the feasibility of such an initiative depends on the long-term availability and variability of water resources within the catchment, making hydroclimatic assessment a prerequisite for sustainable planning. Accurate assessment of hydroclimatic conditions is therefore essential for reservoir management. Reanalysis products such as MERRA-2 provide valuable long-term climate information in regions where observational records are limited (Rienecker et al., 2011; Gelaro et al., 2017). Several studies have demonstrated the usefulness of MERRA-2 and other global datasets for hydrological applications, including precipitation and water balance assessments (Reichle et al., 2017; Bosilovich et al., 2017; Sun et al., 2018). However, previous research has also highlighted important uncertainties in reanalysis-based precipitation and evaporation estimates, particularly at local scales where climatic and topographic effects are insufficiently represented (Nkiaka et al., 2017; Tian et al., 2018; Martens et al., 2017). Furthermore, recent studies emphasize that traditional trend detection methods such as the Mann–Kendall test and Sen's slope may not fully capture complex hydroclimatic changes, suggesting the need for more comprehensive analytical approaches (Zhou et al., 2023; Kartal & Muratoglu, 2026).

Despite these advances, limited information exists regarding the hydroclimatic behaviour of the Kalamu catchment, the reliability of MERRA-2 data for supporting local water resource management, and the potential hydrological conditions required for future mini-hydropower development, representing important research gaps.

The present study aims to evaluate the hydroclimatic variability of the Kalamu catchment and its implications for water availability at the Kalamu intake dam during the period 1992–2023. Specifically, the study assesses the agreement between observed and MERRA-2 precipitation and evaporation data, analyses long-term hydroclimatic trends, classifies hydrological years according to wet, normal, and dry conditions, evaluates the water balance dynamics of the basin, determines the implications of potential water deficits for reservoir operation and water supply sustainability, and provides preliminary information relevant to assessing the future feasibility of small-scale hydropower development at the Kalamu dam. To achieve these objectives, monthly precipitation and evaporation observations from the Boma meteorological station were combined with MERRA-2 reanalysis data covering the period 1992–2023. Statistical performance indicators, including Pearson correlation, coefficient of determination (R^2), Mean Absolute Error (MAE), Root Mean Square Error (RMSE), and bias, were used to evaluate the agreement between datasets (Hodson, 2022). Hydroclimatic variability was investigated through water balance analysis and hydrological year classification using the Z-score method. Long-term trends were assessed using the Mann–Kendall test and Sen's slope estimator (Zakwan & Ahmad, 2021; Zhou et al., 2023). The integrated analysis provides a scientific basis for improving water resources management, evaluating the sustainability of water supply, and supporting future assessments of mini-hydropower potential at the Kalamu intake dam under current and future climatic conditions.

2. Materials and methods

2.1 Presentation of the study environment

The Kalamu Dam (5.81°S, 13.08°E), located in the city of Boma in Kongo Central Province, Democratic Republic of the Congo (Figure 1), was constructed in 1903 on the Kalamu River to provide a gravity-fed water supply to the city through an intake station with a capacity of 67 $m^3\ h^{-1}$. The reservoir has a storage capacity of approximately 160 m^3 and the surface area is 100 m^2. However, the Kalamu River frequently dries up during the dry season, making water abstraction impossible. In addition, the reservoir is extensively covered by algae and exhibits advanced eutrophication, which further threatens water quality and the sustainability of the water supply system for which the Kalamu catchment station was abandoned (Mampuya et al., 2026).

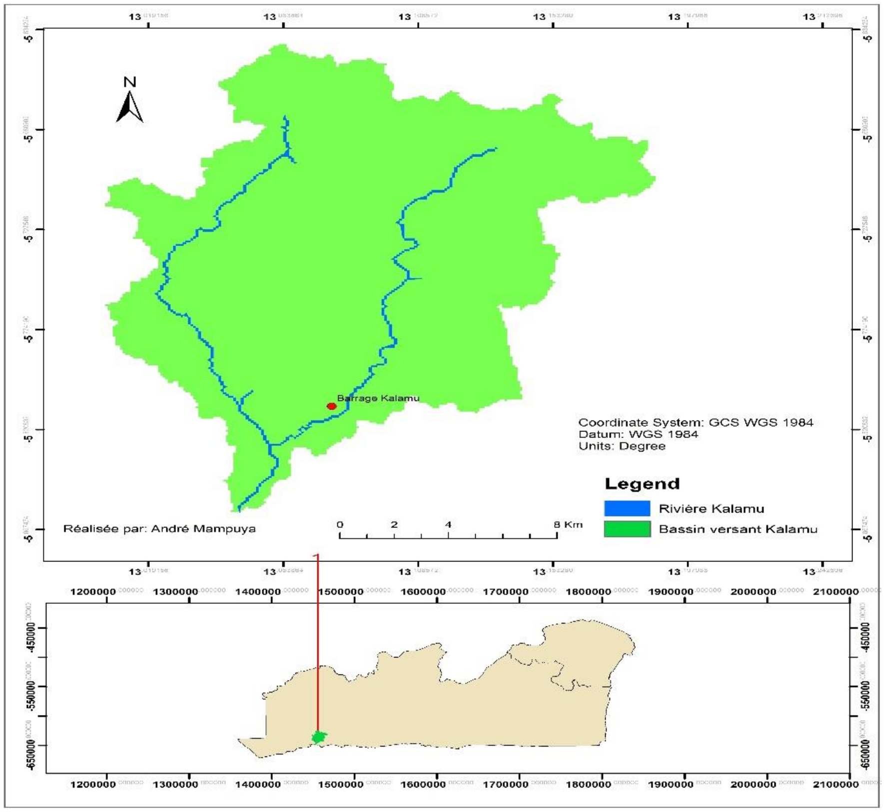

Figure 1. Kalamu River watershed at Boma

2.2. Data collection

Crucial hydroclimatic data were collected from multiple sources. Monthly precipitation and evaporation observations for the period 1992–2023 were obtained from the Boma Meteorological Station. In addition, gridded precipitation and evaporation data covering the Kalamu Dam catchment for the same period (1992–2023) were extracted from the MERRA-2 (Modern-Era Retrospective Analysis for Research and Applications, Version 2) reanalysis dataset. MERRA-2 provides globally consistent atmospheric and land-surface variables and has been widely used for hydrological and climate studies (Rienecker et al., 2011; Gelaro et al., 2017; Reichle et al., 2017; Bosilovich et al., 2017). The combined use of ground-based observations and reanalysis products enables a comprehensive assessment of hydroclimatic variability and water balance dynamics in the Kalamu catchment (Sun et al., 2018; Nkiaka et al., 2017).

2.3. Data analysis

2.3.1 Precipitation or evaporation comparison data station methodology of Boma and MERRA-2 Reanalyzed in Anaconda (Python Environment)

The methodological pipeline begins with the setup of a scientific computing environment using Anaconda, which integrates essential data science libraries, including NumPy, Pandas, Matplotlib, Seaborn, SciPy, and Scikit-learn for data processing, visualization, and statistical analysis (Mampuya et al., 2026; Mampuya Nzita et al., 2025). Observed precipitation or evaporation data from the Boma meteorological station and simulated data from the MERRA-2 reanalysis are structured into numerical arrays. Both datasets are then synchronized using a continuous monthly time index generated via Pandas’ date-range function to ensure strict temporal alignment for subsequent paired statistical analyses (Bosilovich et al., 2017; Gelaro et al. 2017).

Once the datasets are harmonized, the analysis proceeds to statistical evaluation. The first diagnostic metric is the Pearson correlation coefficient, which measures the linear association between observed and simulated precipitation. Mathematically, it is defined as (Dezfuli et al., 2017):

$$r = \frac{\sum(x_i-\bar{x})(y_i-\bar{y})}{\sqrt{\sum(x_i-\bar{x})^2\sum(y_i-\bar{y})^2}} \quad (1)$$

This coefficient provides a normalized measure of covariability between the two datasets, ranging from −1 to +1, and indicates the degree of linear agreement between observation and reanalysis outputs. A value close to +1 suggests strong positive correspondence, while values near zero indicate weak or no linear relationship (Mampuya et al., 2026; Mampuya Nzita et al., 2025).

The coefficient of determination is then derived as the square of the Pearson correlation, expressed as $R^2 = r^2$, which quantifies the proportion of variance in observed precipitation or evaporation that is explained by the MERRA-2 dataset. This metric is widely used in regression-based validation studies because it provides an interpretable measure of explanatory power within the model framework (Nkiaka et al., 2017).

To evaluate systematic deviations between datasets, the bias is computed as the arithmetic mean of differences between simulated and observed precipitation values (Nkiaka et al., 2017; Wang et al., 2023):

$$Bias = \frac{1}{n}(y_{sim} - y_{obs}) \quad (2)$$

This measure identifies whether the reanalysis product systematically overestimates or underestimates precipitation relative to ground observations (Mampuya et al., 2026; Mampuya Nzita et al., 2025). In climatological validation, bias is a critical indicator of systematic model error.

The robustness of the model performance is further assessed using two complementary error metrics. The root mean square error (RMSE) is defined as (Hodson, 2022):

$$RMSE = \sqrt{\frac{1}{n}\sum(y_{sim} - y_{obs})^2} \quad (3)$$

RMSE quantifies the standard deviation of prediction errors and gives greater weight to large deviations due to the squaring operation, making it particularly sensitive to extreme discrepancies (Hodson, 2022; Mampuya et al., 2026; Mampuya Nzita et al., 2025).

In parallel, the mean absolute error (MAE) is defined as (Hodson, 2022) :

$$MEA = \frac{1}{n}\sum|y_{sim} - y_{obs}| \quad (4)$$

Unlike RMSE, MAE provides a linear average of absolute deviations, offering a more robust measure of typical error magnitude that is less influenced by outliers (Hodson, 2022; Mampuya et al., 2026; Mampuya Nzita et al., 2025).

To further characterize the relationship between the two datasets, a simple linear regression model is fitted using the least-squares method, expressed as y = ax + b. In this formulation, the slope and intercept are estimated using NumPy’s polynomial fitting function, enabling the identification of systematic scaling differences between observed and simulated precipitation (Dezfuli et al., 2017; Hodson, 2022; Wang et al., 2023). Finally, the methodological framework incorporates comprehensive visualization techniques to support interpretation. Time series plots are used to assess temporal variability and seasonality, scatter plots with identity and regression lines are used to evaluate agreement and systematic deviation, histograms are used to examine error distributions, boxplots describe statistical dispersion, and monthly climatologies highlight seasonal consistency between datasets.

2.3.2. Climatic and Hydrological Analysis of the Boma Meteorological Station for the Kalamu Dam Using Python (Anaconda)

This analysis was carried out in the Python Anaconda environment using the Pandas, NumPy, SciPy, Matplotlib, and Seaborn libraries (Nzita et al., 2025; Mampuya et al., 2026; Mampuya Nzita et al., 2025). The main objective is to assess the evolution of precipitation, evaporation, and water balance over the period 1992–2023 and to detect potential climatic trends using the Mann–Kendall test and Sen's slope (Theil–Sen estimator), two widely used non-parametric methods in hydrology and climatology (Zakwan and Ahmad, 2021).
At the beginning of the analysis, monthly precipitation and evaporation time series are organized into a DataFrame indexed from January 1992 to December 2023. Each row represents a monthly observation containing precipitation (mm/month) and evaporation (mm/day).
Since evaporation data are expressed in millimeters per day, they must be converted into monthly values by multiplying the daily mean evaporation by the number of days in each month (McMahon et al., 2013; Tian et al., 2018; Martens et al., 2017):

$$E_m = E_d \times N_d \quad (5)$$

Where E_m is monthly evaporation (mm/month), E_d is daily evaporation (mm/day), and N_d is the number of days in the month.
Once evaporation is converted into monthly values, the climatic water balance is calculated. The water balance represents the difference between received precipitation and losses due to evaporation. It is expressed as (Bosilovich et al., 2017; Xiong et al., 2023; Hou et al., 2022) :

$$BH = P - E_m \quad (6)$$

Where BH is the water balance (mm), P is monthly precipitation (mm), and E_m is monthly evaporation (mm).

When:

$$\begin{cases} BH > 0 \ \rightarrow the\ system\ shows\ a\ water\ surplus \\ BH < 0 \ \rightarrow the\ system\ shows\ a\ water\ deficit \end{cases} \quad (7)$$

To analyse climatic fluctuations around the long-term mean, anomalies are computed for each variable. An anomaly is defined as the deviation between an individual observation and the long-term mean of the dataset (Xiong et al., 2023; Hou et al., 2022; McMahon et al., 2013).
For precipitation:

$$A_P = P_i - \bar{P} \quad (8)$$

For evaporation :

$$A_E = E_i - \bar{E} \quad (9)$$

For water balance :

$$A_{BH} = BH_i - \overline{BH} \quad (10)$$

Where P_i, E_i et BH_i are observed values and $\bar{P}$, $\bar{E}$ et $\overline{BH}$ are long-term means (1992–2023). A positive anomaly indicates above-average conditions, while a negative anomaly indicates below-average conditions. Afterwards, the data are aggregated at an annual scale using (Degefu et al., 2024; Alemu et al., 2025) :

$$annual = df.resample\,('y').sum() \quad (11)$$

This produces annual precipitation totals, evaporation totals, and water balance values.

To identify wet and dry years, the Z-score method is applied (Miller et al.,2021; Balme et al., 2006) :

$$Z = \frac{X-\mu}{\sigma} \quad (12)$$

Where X is the annual value, μ is the mean, and σ is the standard deviation.

Classification rules are:

$$\begin{cases} Z > 1 \rightarrow wet\ year \\ Z < 1 \rightarrow dry\ year \\ -1 \leq Z \leq 1 \rightarrow normal\ year \end{cases} \quad (13)$$

This method allows rapid identification of hydrological extremes.

Finally, trend detection is performed using the Mann–Kendall test based on Kendall's tau (τ), which is well suited for hydrological time series without requiring normal distribution (Zhou et al., 2023). The test compares all possible pairs of observations. The test statistic S is defined as (Zakwan and Ahmad, 2021):

$$S = \sum_{i=1}^{n-1} \sum_{j=i+1}^{n} sgn(X_j - X_i) \quad (14)$$

Where (Zakwan et Ahmad, 2021) :

$$sgn(X_j - X_i) = \begin{cases} +1 \quad si\ X_j - X_i > 0 \\ 0 \quad si\ X_j - X_i = 0 \\ -1 \quad si\ X_j - X_i < 0 \end{cases} \quad (15)$$

A positive value of **S** indicates an increasing trend, whereas a negative value indicates a decreasing trend (Zhou et al., 2023).

In the script, this procedure is simplified using kendall τ (x, variable), which directly provides both the τ coefficient and the corresponding p-value.

The statistical hypotheses are (Zhou et al., 2023):

$$\begin{cases} H_0: absence\ of\ trend \\ H_1: presence\ of\ a\ trend \end{cases} \quad (16)$$

The decision rule is as follows (Zhou et al., 2023):

$$\begin{cases} p < 0.05 \rightarrow \text{significant trend} \\ p > 0.05 \rightarrow \text{non significant trend} \end{cases} \quad (17)$$

Once significance is established, the magnitude of the trend is estimated using Sen's slope (Theil–Sen estimator). This method computes all possible pairwise slopes between observations (Zakwan and Ahmad, 2021):

$$Q_{ij} = \frac{X_j - X_i}{j-i} \quad (18)$$

Where j>i (for i=1,2,3,…,n). Sen's slope is then obtained as the median of all calculated pairwise slopes (Zakwan and Ahmad, 2021):

$$Q_{sen} = median\left(\frac{X_j - X_i}{j-i}\right) \quad (19)$$

With

$$\begin{cases} if\ Q_{sen} > 0 \rightarrow the\ trend\ is\ increasing \\ if\ Q_{sen} < 0 \rightarrow the\ trend\ is\ decreasing \end{cases}$$

This method is robust to extreme values and is widely used in hydrology to quantify the rate of change of a climatic variable (Kartal and Muratoglu, 2026). In the function theilslopes (variable, x, 0.95), Sen's slope, the intercept, and the lower and upper bounds of the confidence interval are returned. The study then focuses on water deficits, which are calculated when evaporation exceeds precipitation (Xiong et al., 2023):

$$D = E_m - P \quad (20)$$

Only positive values are retained:

$$D = max(E_m - P, 0) \quad (21)$$

The deficits are then converted into meters (Hou et al., 2022; Xiong et al., 2023):

$$D_m = \frac{D}{100} \quad (22)$$

Then in volume of water (Hou et al., 2022; Fernández-Pato et al., 2016) :

$$V_D = D_m \times A \quad (23)$$

Where A = 68.8 km² = 68800000 m² is the catchment area of the Kalamu watershed, and the sub-basin near the Kalamu dam has an area of 538.8 m².
The total deficit volume is obtained as (Hou et al., 2022; Fernández-Pato et al., 2016):

$$V_{total} = \sum V_D \quad (24)$$

This value represents the theoretical volume of water required to compensate for all deficits observed over the study period. For reservoir sizing purposes, annual deficit volumes are summed, and the maximum annual deficit is retained as the design reference. The relationship is expressed as (Hou et al., 2022; Fernández-Pato et al., 2016) :

$$V_{reservoir} = max(\sum V_D) \quad (25)$$

This value represents the minimum recommended reservoir capacity required to meet water demand during the most water-deficient year. The analysis also distinguishes two hydrological seasons: a wet season and a dry season. Each monthly observation is classified according to its date. Seasonal statistics are then computed based on the mean values of precipitation, evaporation, and water balance (Balme et al., 2006; Alahacoon et al., 2022 ; Seager et al., 2019):

$$\bar{X}_{\text{season}} = \frac{\sum X_i}{n} \quad (26)$$

Finally, a monthly climatology is generated by calculating the mean value for each month over the entire 32-year study period (Alahacoon et al., 2022; Degefu et al., 2024; Alemu et al., 2025):

$$Clim_{month} = \frac{\sum X_{month}}{n} \quad (27)$$

Where n represents the number of available years in the dataset. The results are subsequently visualized through annual time series, water balance anomalies, monthly climatologies, seasonal boxplots, and trend curves derived from Sen's slope estimator. The resulting datasets and statistical outputs are finally exported to Excel format to facilitate interpretation, reporting, and integration into scientific analyses.
From a scientific perspective, this methodology combines three complementary levels of analysis: descriptive climate analysis based on long-term averages and anomalies, statistical trend assessment using the Mann–Kendall test and Sen's slope estimator, and hydrological evaluation of water deficits for reservoir storage design and management purposes. This integrated framework is widely

recognized as a robust and reliable approach for long-term hydroclimatic studies (Zakwan and Ahmad, 2021).

3. Results and Discussion

3.1. Comparative Analysis of Observed and MERRA-2 Reanalysis Monthly Precipitation Patterns at Kalamu Water Intake Dam (1992–2023)

Figure 2 illustrates the temporal variability, mean monthly precipitation patterns, and statistical distribution of precipitation estimates, providing insights into the consistency and representativeness of the MERRA-2 reanalysis product relative to ground-based observations.

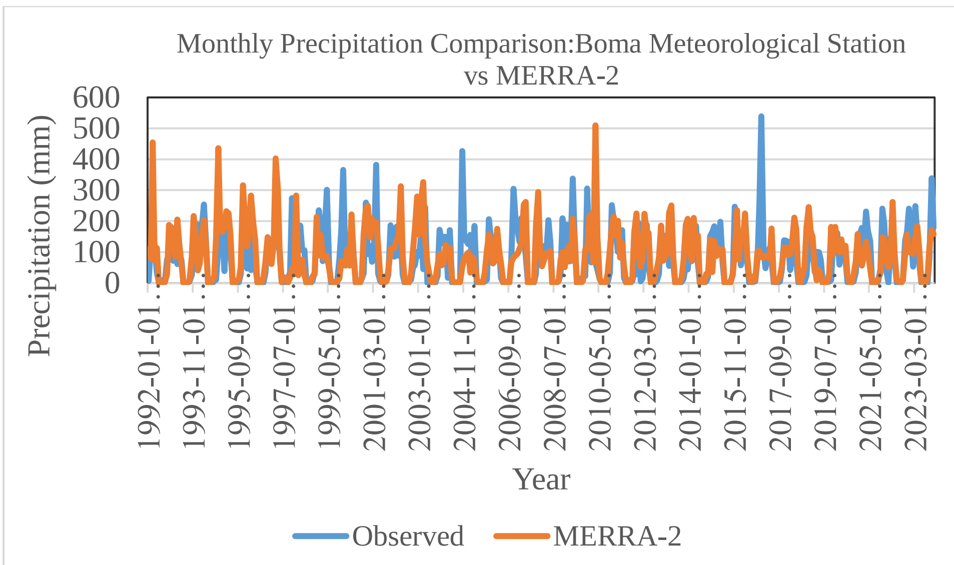

a) Comparative analysis of monthly precipitation time series derived from ground observations and MERRA-2 reanalysis data

Figure 2. Comparative evaluation of observed and MERRA-2 Monthly Precipitation at Boma Meteorological Station (1992–2023)

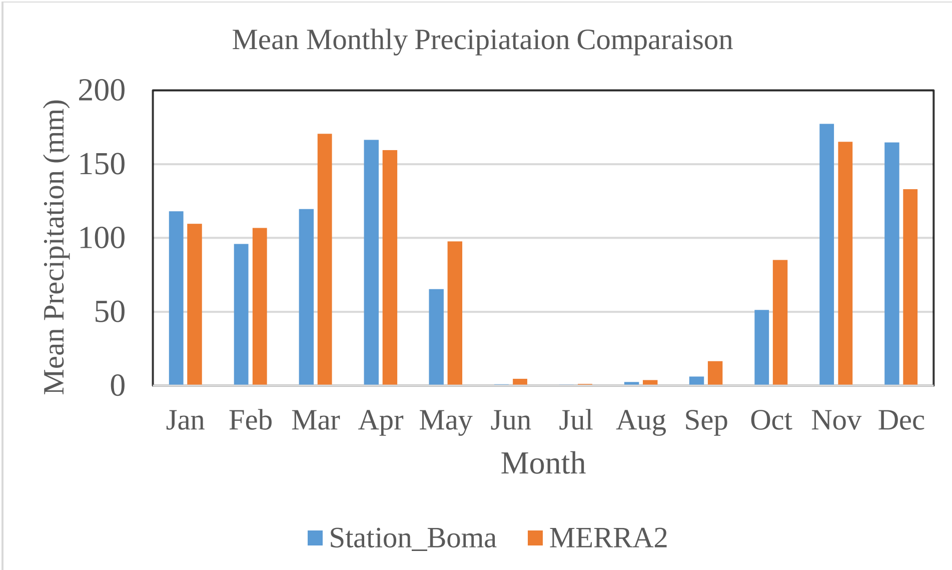

b) Comparison of mean monthly precipitation patterns between observed records and MERRA-2 estimates

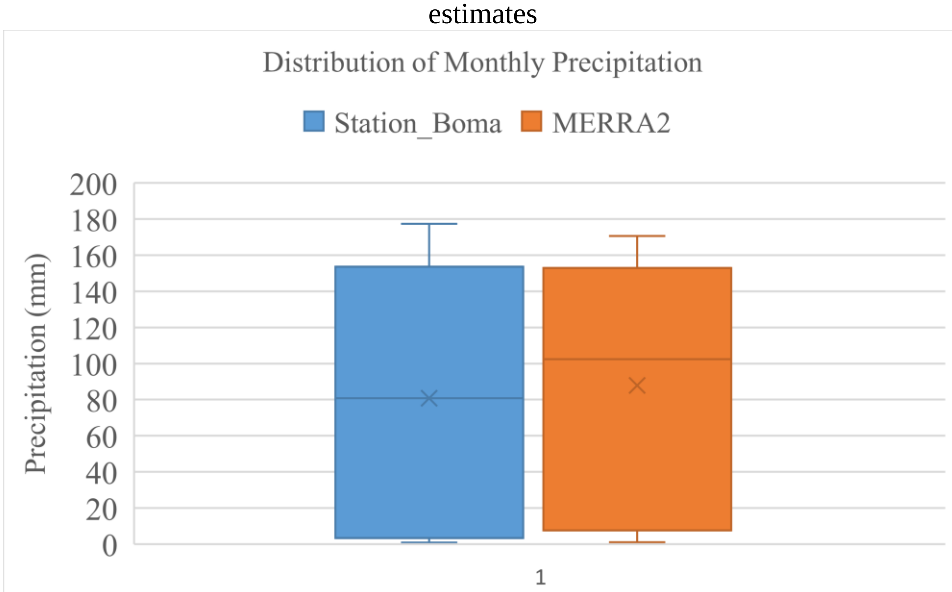

c)Distribution of monthly precipitation values from observations and MERRA-2 reanalysis over the study period

Figure 2 (continued). Comparative evaluation of observed and MERRA-2 Monthly Precipitation at Boma Meteorological Station (1992–2023)

Figure 2a shows that both datasets describe similar mean rainfall conditions: 80.8 mm (station) versus 87.9 mm (MERRA-2), indicating a small overestimation of about +7 mm/month by the model. Extreme rainfall is also comparable (538.9 mm vs 509.6 mm), and variability is nearly identical (standard deviation: 85.1 mm vs 85.7 mm), confirming consistent representation of wet and dry fluctuations.

Figure 2b illustrates a shared seasonal cycle, with a wet season from October to May and a dry season from June to August. Peak rainfall occurs in

November, December, March, and April. MERRA-2 slightly overestimates rainfall in transitional months (March, May, September, October), while the station records higher values in November and December.

Figure 2c confirms similar distributions: close medians, near-zero minima indicating a strong dry season, and comparable spread. However, observed extremes are higher than modeled ones, meaning MERRA-2 slightly smooths intense rainfall events. Overall, the model reliably reproduces local rainfall dynamics.

3.2. Statistical Agreement and Error Characterization Between Observed and MERRA-2 Monthly Precipitation Data at Boma Meteorological Station (1992–2023)

The evaluation of precipitation shows moderate agreement between MERRA-2 and station data. The Mean Absolute Error (MAE = 53.14 mm) indicates an average monthly difference of about 53 mm, while the higher RMSE (85.71 mm) suggests that large errors occur during heavy rainfall events. The coefficient of determination ($R^2 = 0.25$) shows that only 25% of observed rainfall variability is explained by MERRA-2, meaning the model captures general trends but not local rainfall fluctuations driven by factors such as relief and storms. The positive bias of +7.05 mm (+8.73%) indicates a slight overall overestimation of rainfall. Overall, Figure 3 shows that MERRA-2 is useful for identifying broad climatic patterns but less accurate for detailed local precipitation variability.

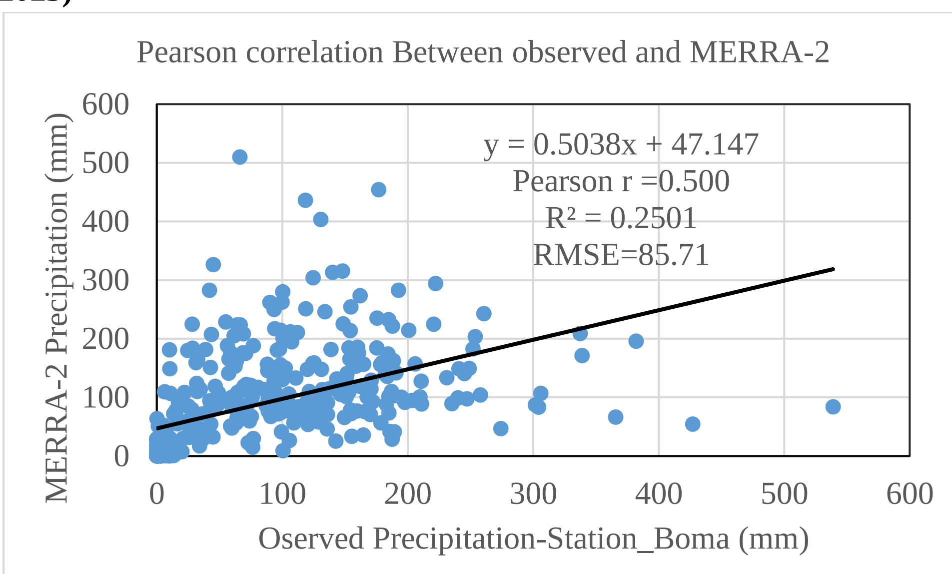

a) Linear regression and Pearson correlation analysis between observed monthly precipitation at Boma Meteorological Station and MERRA-2 reanalysis estimates

Figure 3. Statistical Evaluation of the Agreement Between Observed and MERRA-2 Monthly Precipitation at Boma Meteorological Station (1992–2023)

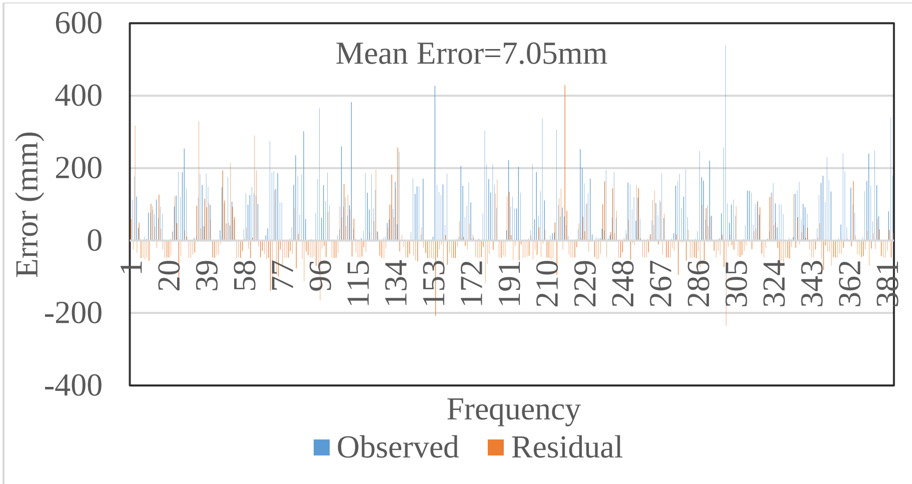

b) Error distribution of MERRA-2 monthly precipitation estimates relative to ground-based observations at Boma Meteorological Station

Figure 3 (continued). Statistical Evaluation of the Agreement Between Observed and MERRA-2 Monthly Precipitation at Boma Meteorological Station (1992–2023)

Figure 3a shows the relationship between observed rainfall at Boma (x) and MERRA-2 estimates (y). The blue points represent paired values, while the green line indicates perfect agreement. The dispersion around this line shows a moderate but imperfect match between both datasets. The Pearson correlation coefficient (r = 0.50) indicates a moderate positive relationship, meaning that when rainfall increases at Boma, MERRA-2 generally increases as well. The relationship is statistically significant ($p \approx 0.00000$). The linear regression equation is:

$$y = 50x + 47.15 \quad (28)$$

Here, x is observed rainfall (mm) and y is MERRA-2 rainfall (mm). The slope (0.50) means that a 100 mm increase at the station corresponds to only a 50 mm increase in MERRA-2, showing that the model smooths extreme rainfall. The intercept (47.15 mm) indicates that MERRA-2 still estimates rainfall even when observed rainfall is near zero, explaining a positive bias.

Figure 3b presents the error distribution (MERRA-2 minus station). Most values cluster near zero, indicating frequent agreement between both datasets. However, the mean error of +7.05 mm shows a systematic overestimation by MERRA-2. Occasional large deviations indicate rare but significant mismatches. Overall, MERRA-2 captures general rainfall variability but smooths extremes and slightly overestimates precipitation, making it useful for trend analysis but less precise for event-scale study.

3.3. Comparative Analysis of Observed and MERRA-2 Reanalysis Monthly evaporation Patterns at Kalamu Water Intake Dam (1992–2023)

The figure 2 illustrates the temporal variability, mean monthly precipitation patterns, and statistical distribution of evaporation estimates, providing insights into the consistency and representativeness of the MERRA-2 reanalysis product relative to ground-based observations.

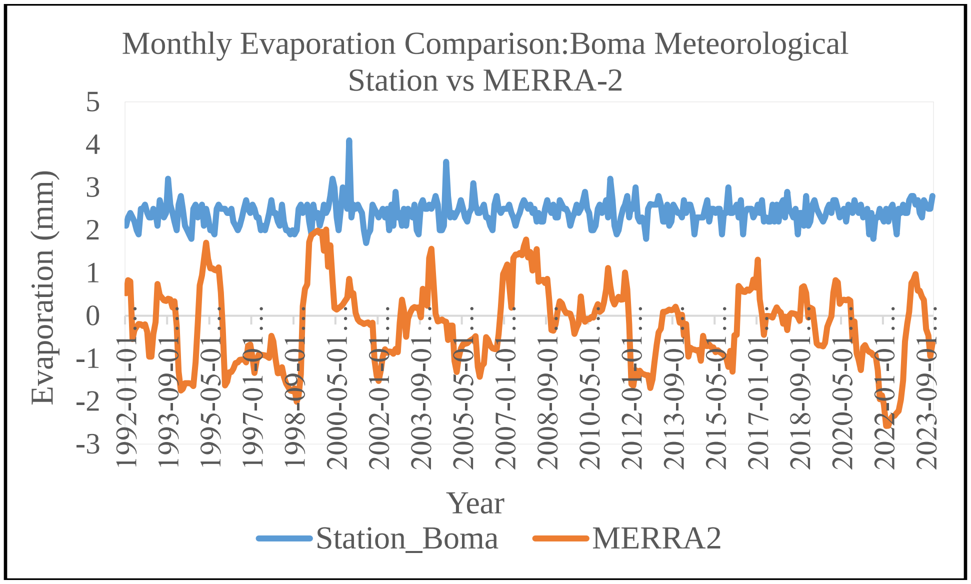

a) Comparative analysis of monthly evaporation time series derived from ground observations and MERRA-2 reanalysis data

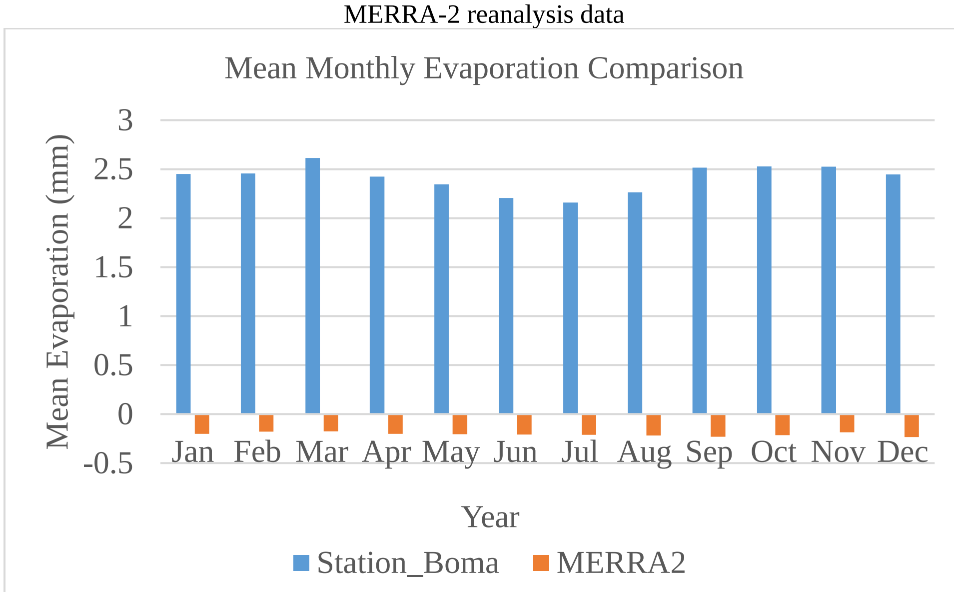

b) Comparison of mean monthly evaporation patterns between observed records and MERRA-2 estimates

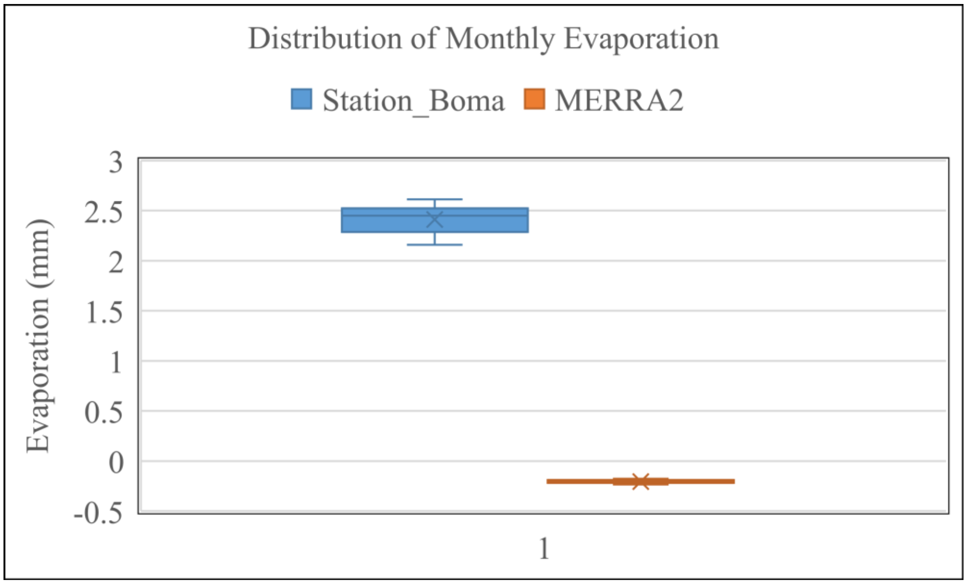

c) Distribution of monthly evaporation values from observations and MERRA-2 reanalysis over the study period

Figure 4. Comparative evaluation of observed and MERRA-2 Monthly evaporation at Boma Meteorological Station (1992–2023)

Figure 4a shows that the Boma station records consistent evaporation values ranging from 1.70 to 4.10 mm, with a mean of 2.41 mm and low variability (SD = 0.27), indicating stable monthly behavior. In contrast, MERRA-2 produces a mean of −0.21 mm, minimum values down to −2.58 mm, and higher variability (SD = 0.92). These negative values are physically unrealistic and indicate a systematic underestimation of evaporation.

Figure 4b compares monthly means and clearly shows that MERRA-2 strongly underestimates evaporation in all months. While the station remains around 2.0–2.6 mm/month, MERRA-2 values are near zero or much lower, meaning the model fails to capture real evaporative water loss dynamics.

Figure 4c confirms this pattern through distribution analysis: the station shows a stable central range around ~2.2–2.6 mm, while MERRA-2 is widely dispersed and centered near zero. Overall, MERRA-2 does not reliably represent evaporation and may lead to underestimating water losses if used without correction.

3.2. Statistical Agreement and Error Characterization Between Observed and MERRA-2 Monthly evaporation Data at Boma Meteorological Station (1992–2023)

The statistical evaluation shows clear differences between MERRA-2 and station-based evaporation data. The Mean Absolute Error (MAE = 2.617 mm) indicates an average deviation of about 2.6 mm between both datasets, while the RMSE (2.775 mm) confirms relatively consistent errors. The coefficient of determination (R^2 = 0.019) means that only 1.9% of the observed variability at Boma is explained by MERRA-2, showing very weak performance in capturing local evaporation dynamics. In addition, the bias of −2.617 mm (−108.51%) reveals a systematic underestimation of evaporation by the model. Overall, Figure 5 demonstrates that, despite using regression, correlation, and error analysis, MERRA-2 has limited reliability for accurately representing local evaporation variability and should be used cautiously in hydrological assessments.

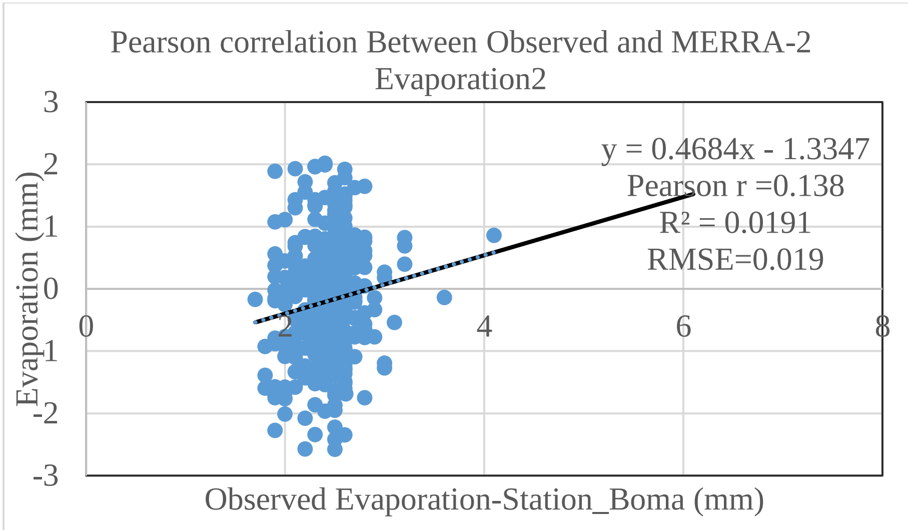

a) Linear regression and Pearson correlation analysis between observed monthly evaporation at Boma Meteorological Station and MERRA-2 reanalysis estimates

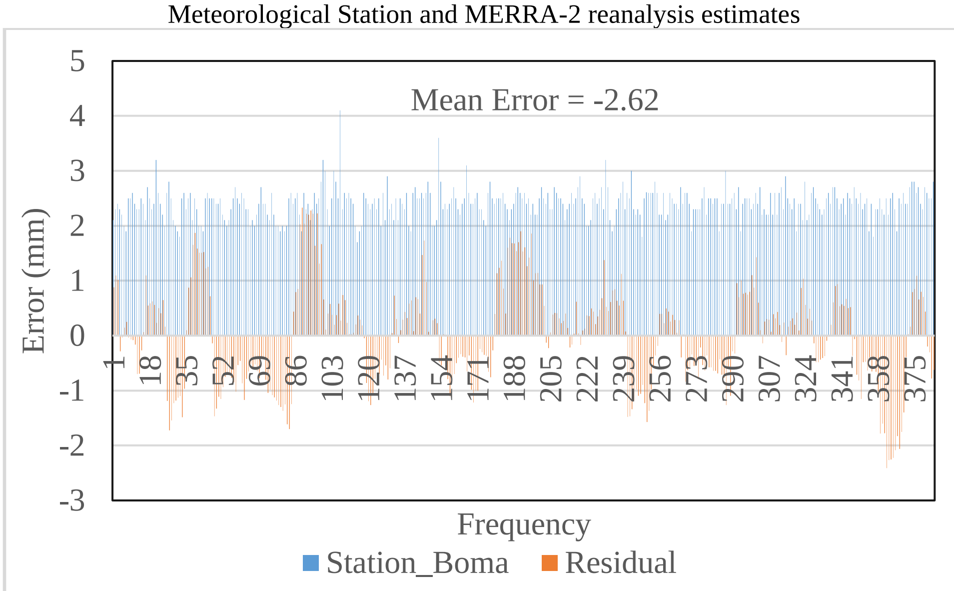

b) Error distribution of MERRA-2 monthly evaporation estimates relative to ground-based observations at Boma Meteorological Station

Figure 5. Statistical Evaluation of the Agreement Between Observed and MERRA-2 Monthly evaporation at Boma Meteorological Station (1992–2023)

Figure 5a shows a weak agreement between observed evaporation at Boma (x) and MERRA-2 estimates (y). The blue points are widely scattered around the regression line and often deviate from the reference line, indicating poor reproduction of observed variability. The Pearson correlation coefficient (r = 0.138) confirms a very weak positive

relationship, although it remains statistically significant (p = 0.00671).
The linear regression equation is:

$$y = 0.47x - 1.33 \quad (29)$$

Here, x represents observed evaporation (mm) and y represents MERRA-2 evaporation (mm). The slope (0.47) indicates that a 1 mm increase in observed evaporation corresponds to only a 0.47 mm increase in MERRA-2, showing strong damping of variability. The negative intercept (−1.33 mm) means the model can produce unrealistic low values when observations are near zero, confirming a systematic underestimation. Figure 5b presents the error distribution (MERRA-2 minus station). Most values cluster between approximately −5 and 0 mm, meaning MERRA-2 generally underestimates evaporation. The mean error of −2.62 mm confirms this systematic negative bias. While small errors occur frequently, larger negative deviations highlight periods of significant mismatch. Overall, MERRA-2 captures only weakly the observed evaporation dynamics and should be used cautiously for water balance studies.

3.3. Hydroclimatic Variability, Hydrological Year Classification, and Water Balance Trend Analysis

Table 1 presents the classification of hydrological years at the Boma meteorological station (1992–2023) using the Z-score method. It identifies wet, normal, and dry years, providing a concise overview of rainfall variability and periods of water surplus or deficit affecting the Kalamu catchment.

Table 1. Identification des années hydrologiques selon le test du Z-score à la station météorologique de Boma (1992–2023)

Date	Precipitation	P_zscore	Year_Type
1992-12-31	821.2	-0.641798	Normal
1993-12-31	663.7	-1.308905	Dry
1994-12-31	1214.8	1.025332	Wet
1995-12-31	907.0	-0.278384	Normal
1996-12-31	696.1	-1.171671	Dry
1997-12-31	1145.4	0.731381	Normal
1998-12-31	1165.6	0.816940	Normal
1999-12-31	1413.8	1.868215	Wet
2000-12-31	1012.7	0.169318	Normal
2001-12-31	1057.9	0.360767	Normal
2002-12-31	748.2	-0.950997	Normal
2003-12-31	866.9	-0.448232	Normal
2004-12-31	1220.7	1.050322	Wet
2005-12-31	888.7	-0.355896	Normal
2006-12-31	1044.1	0.302316	Normal
2007-12-31	1106.4	0.566193	Normal
2008-12-31	937.8	-0.147928	Normal
2009-12-31	1303.3	1.400182	Wet
2010-12-31	771.5	-0.852308	Normal
2011-12-31	858.8	-0.482540	Normal
2012-12-31	688.3	-1.204709	Dry
2013-12-31	558.8	-1.753218	Dry
2014-12-31	878.3	-0.399946	Normal
2015-12-31	1113.6	0.596689	Normal
2016-12-31	1494.7	2.210874	Wet
2017-12-31	760.0	-0.901017	Normal
2018-12-31	774.8	-0.838330	Normal
2019-12-31	704.4	-1.136516	Dry
2020-12-31	820.5	-0.644763	Normal
2021-12-31	1302.6	1.397217	Wet
2022-12-31	909.8	-0.266525	Normal
2023-12-31	1276.8	1.287938	Wet

Annual precipitation at the Boma meteorological station was analysed using the Z-score method to classify each year (1992–2023) as wet, normal, or dry relative to the long-term mean. This approach highlights interannual rainfall variability and its implications for water supply at the Kalamu water intake dam. Wet years are identified when the Z-score is above +1, indicating rainfall significantly higher than average. These include 1994, 1999, 2004, 2009, 2016, 2021, and 2023. During such years, inflows to the dam were likely enhanced, improving reservoir filling and water availability. The most extreme case is 2016, with 1,494.7 mm of rainfall and a Z-score of 2.21, reflecting exceptionally wet conditions. Dry years occur when the Z-score is below −1, indicating rainfall deficits. These include 1993, 1996, 2012, 2013, and 2019. In particular, 2013 recorded only 558.8 mm with a Z-score of −1.75, marking a severe drought that could reduce water supply reliability. Most years (about 62.5%) fall within the normal range (−1 to +1), meaning rainfall close to the long-term average and generally stable hydrological conditions. These years support relatively balanced dam operation without major surplus or shortage. Overall, the results show a climate dominated by normal conditions but interrupted by occasional wet and dry extremes. This variability directly affects water availability at the Kalamu dam and highlights the need for adaptive water management strategies.

Figure 6 presents hydroclimatic variability at Boma station (1992–2023), showing annual, monthly, and seasonal changes in precipitation, evaporation, and water balance. It highlights fluctuations between wet and dry periods and their influence on the hydrological dynamics of the Kalamu catchment.

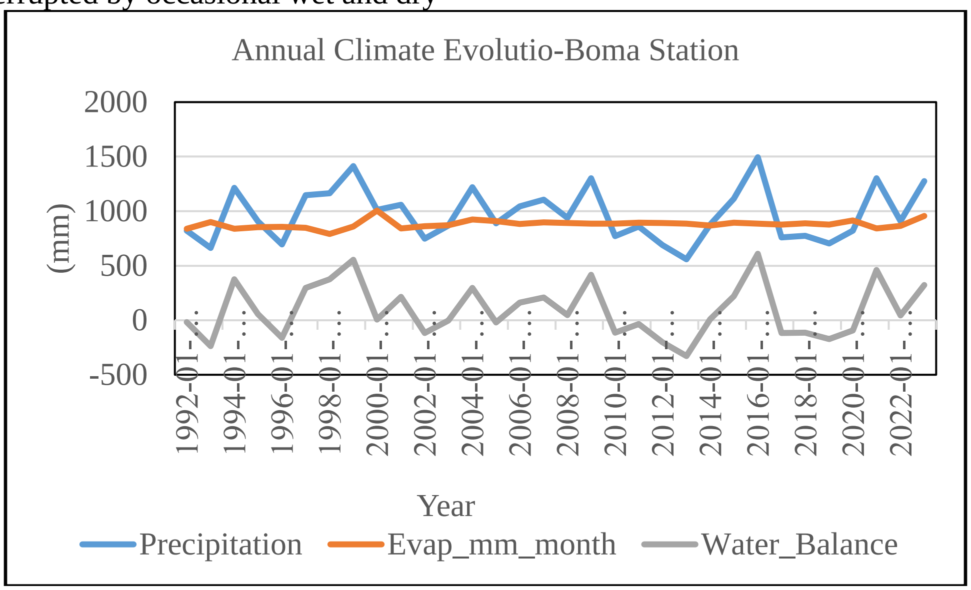

a)Annual evolution of climate variables (precipitation, evaporation, and water balance) at Boma station

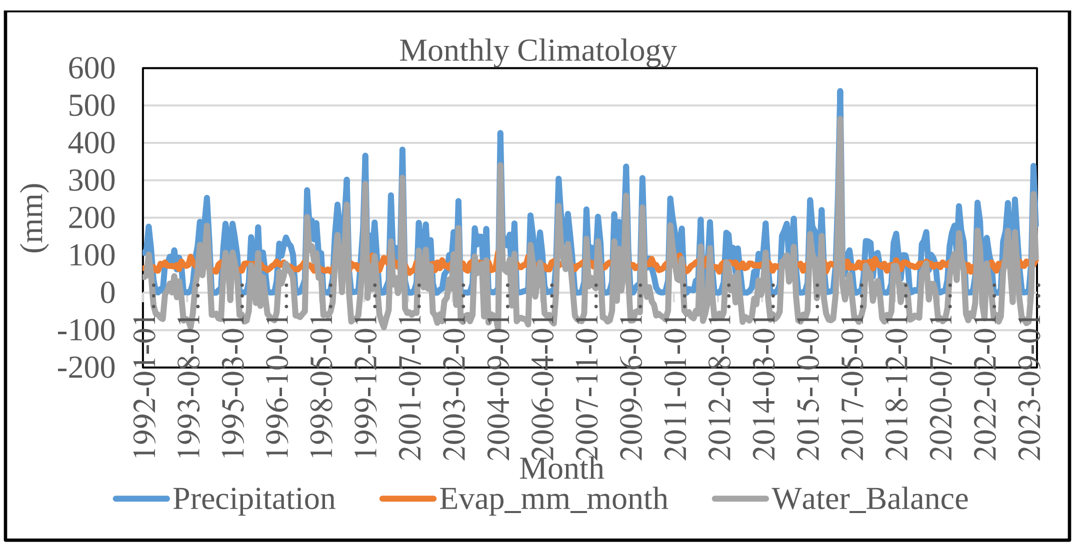

b)Monthly climatology of precipitation, evaporation, and water balance at Boma station

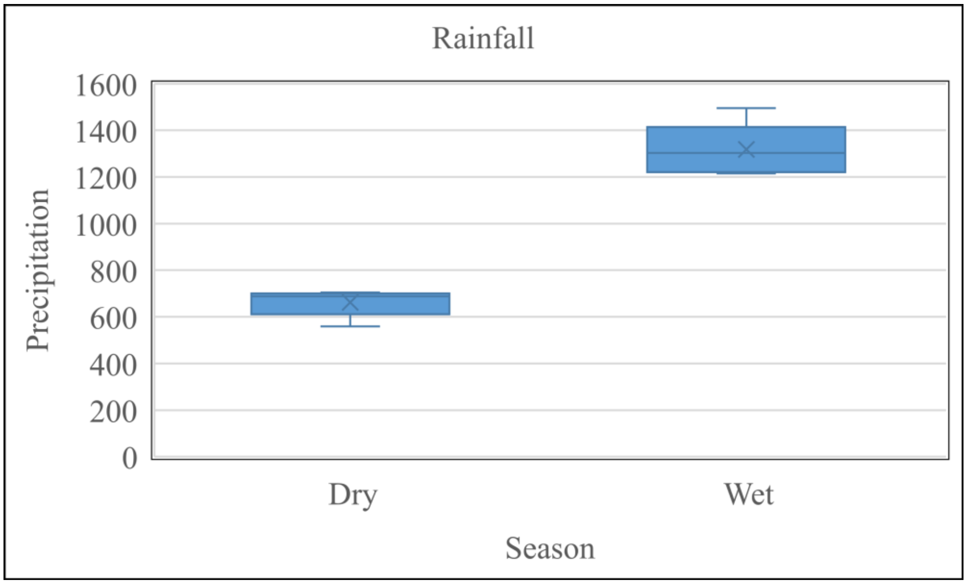

c1) Seasonal boxplot distribution of precipitation

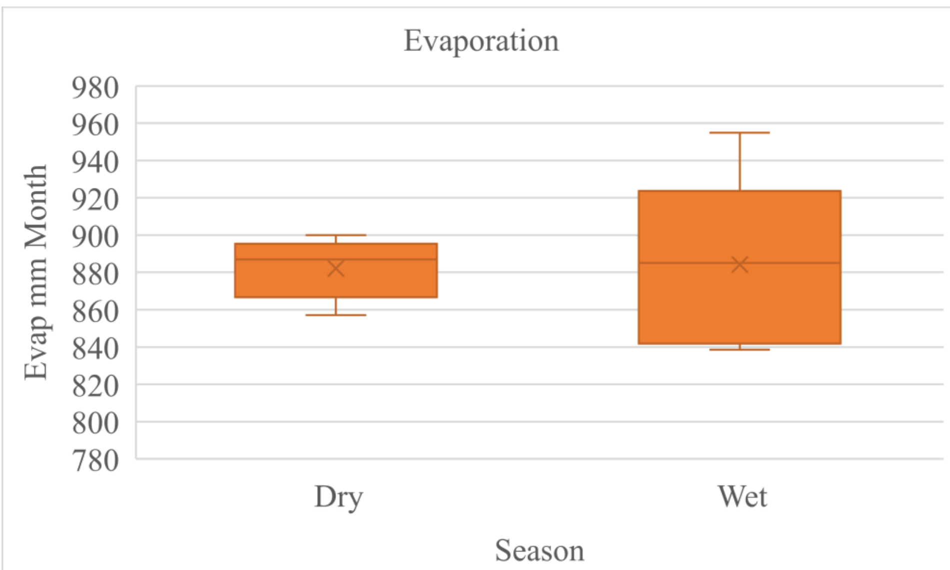

c2) Seasonal boxplot distribution of evaporation

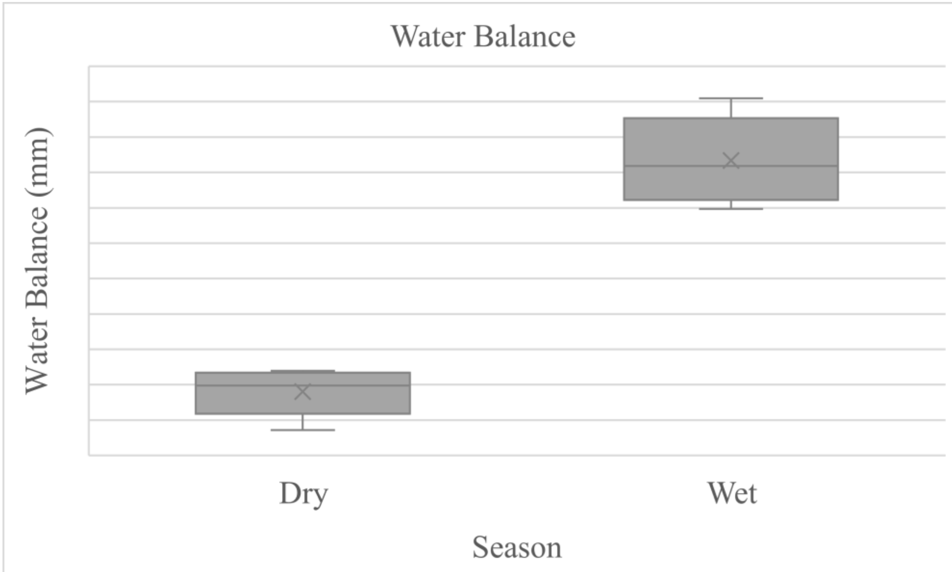

c3) Seasonal boxplot distribution of water Balance

c) Seasonal boxplot distribution of precipitation, evaporation, and water balance comparing wet and dry seasons

Figure 6. Hydroclimatic variability at Boma station (1992–2023)

Figure 6a shows the annual evolution of precipitation, evaporation, and water balance in the Kalamu watershed. Rainfall varies considerably from year to year, reaching more than 1500 mm during wet years, whereas evaporation remains relatively stable between 800 and 1000 mm/year. Consequently, the water balance alternates between surplus and deficit periods, directly influencing water availability for the Kalamu intake dam.

Figure 6b highlights the seasonal cycle. Rainfall peaks during the wet season, particularly in March, while evaporation remains nearly constant at 70–90 mm/month. As a result, the water balance is positive from February to May but becomes negative from June to September when evaporation exceeds rainfall.

Figure 6c confirms these seasonal contrasts. Average rainfall reaches 120.28 mm/month during the wet season but only 2.63 mm/month during the dry season. The average water balance is +45.05 mm/month in the wet season and −67.08 mm/month in the dry season, demonstrating that reservoir recharge occurs mainly during the rainy season while stored water is progressively depleted during dry months.

Figure 7 illustrates the long-term trend of water balance in the Kalamu catchment (1992–2023). It combines annual water balance variations with Sen’s slope analysis, providing an overview of hydrological fluctuations and the overall direction of change in water availability over the study period.

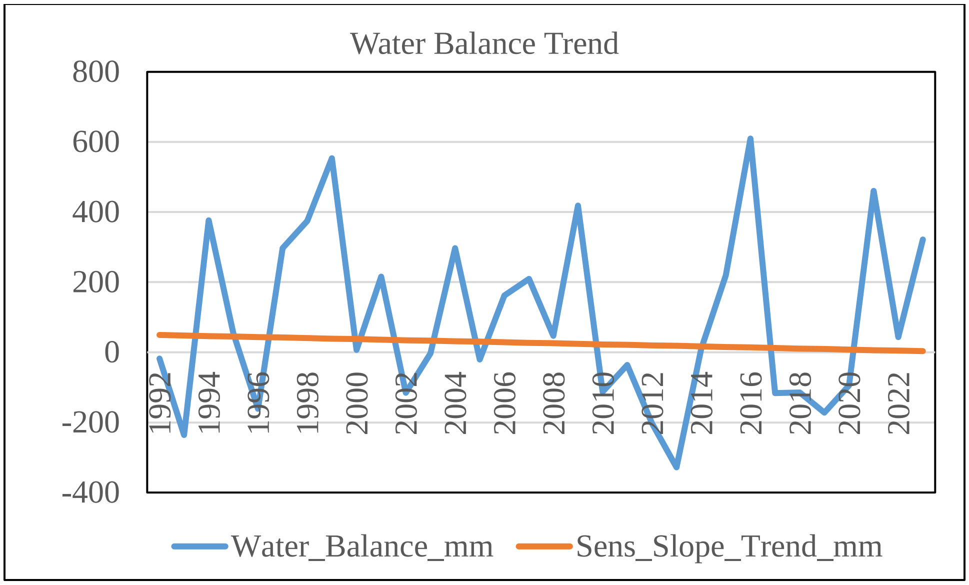

Figure 7. Water Balance Trend (water balance and Sen's slope)

Figure 7 presents the long-term water balance (1992–2023) in the Kalamu River basin at the Boma station. The blue curve shows annual water balance values, while the orange line represents Sen's slope, which indicates the overall trend over time. The water balance fluctuates strongly from year to year. Positive years, such as around 1995, 2000, 2010, and 2015, indicate that precipitation exceeded water losses (mainly evaporation), leading to favourable conditions for reservoir filling and water storage in the Kalamu dam. In contrast, negative years such as 1997, 2005, and 2020 show that water losses were higher than rainfall, which likely reduced water availability in the reservoir and increased the risk of water stress. The Sen's slope line is slightly downward, suggesting a weak long-term decline in the water balance over the 1992–2023 period. However, this downward trend is very small, meaning that no strong or alarming long-term deterioration is observed. In other words, the system remains relatively stable, but with frequent interannual fluctuations between surplus and deficit conditions. Overall, the results indicate that the Kalamu basin experiences alternating wet and dry water balance years, driven by climate variability. While a slight decreasing tendency exists, the main feature of the system is variability rather than a strong long-term trend, which is important for planning sustainable water management at the dam.

Table 2 presents the results of the Mann–Kendall trend test and Sen's slope estimation for key hydroclimatic variables during 1992–2023. It summarizes the direction, magnitude, and statistical significance of long-term changes in precipitation, evaporation, and water balance within the Kalamu catchment.

Table 2. Mann–Kendall Trend Analysis and Sen's Slope Estimation for Hydroclimatic Variables (1992–2023)

Variable	Kendall's Tau (τ)	p-value	Trend Classification	Significant Trend	Sen's Slope (mm/year)
Precipitation	-0.0081	0.96153	No Significant Trend	No	-0.2729
Evaporation	0.2298	0.06658	No Significant Trend	No	1.4515
Water Balance	-0.0484	0.71140	No Significant Trend	No	-1.4879

Table 2 Results of the Mann–Kendall trend test and Sen's slope estimator for precipitation, evaporation, and water balance over the study period (1992–2023). The analysis indicates no statistically significant monotonic trend ($p > 0.05$) for any of the investigated hydroclimatic variables. Although evaporation exhibits a positive Sen's slope, and precipitation and water balance show negative slopes, these trends remain statistically non-significant at the 95% confidence level. The analysis of the Kalamu watershed (1992–2023) shows no statistically significant long-term trend in precipitation, evaporation, or water balance. Rainfall remains relatively stable, with no clear increase or decrease over time, while evaporation shows a slight rise of +1.45 mm/year and water balance a slight decline of −1.49 mm/year. These changes are not yet significant but should be monitored because they could affect future water availability. The main characteristic of the basin is its strong year-to-year variability, with alternating wet and dry years. For the Kalamu dam, there is currently no immediate water crisis, but continuous monitoring and adaptive management are essential to ensure sustainable water resources under future climate change conditions.

The calculated water deficit of 4982.05 m^3 represents the total volume of water lacking to meet the Kalamu basin demand over the studied period, mainly due to insufficient rainfall and/or high evaporation. In practical terms, this indicates that the Kalamu intake dam may not consistently supply enough water, particularly during dry seasons. To compensate for this seasonal deficit, an additional storage capacity of about 209.88 m^3 would be required. However, the current reservoir capacity is 160 m^3, which is slightly below this requirement. This gap means the system has limited ability to store excess water during wet periods for later use in dry periods. As a result, the dam may face water shortages during drought conditions. Improving storage capacity or optimizing water management strategies is therefore necessary to ensure a more stable and reliable water supply throughout the year.

Furthermore, the hydroclimatic results suggest that the installation of a mini-hydropower plant at the Kalamu intake dam is currently not advisable. The observed water deficit, limited storage capacity, seasonal drying of the Kalamu River, and recurrent negative water balance during the dry season indicate insufficient and unreliable water availability to sustain hydropower production without compromising the primary function of the dam, which is water supply. In addition, the absence of a significant long-term increase in precipitation and the slight decline in water balance further reduce the feasibility of hydropower development.

3.4. Comparative Analysis of Observed and MERRA-2 Monthly Precipitation Patterns

The comparison between observed precipitation and MERRA-2 reanalysis reveals a generally coherent representation of the rainfall regime over the Kalamu Water Intake Dam basin, although with systematic biases.

The close agreement in mean monthly precipitation (80.8 mm for observations versus 87.9 mm for MERRA-2) and similar variability confirms that reanalysis products are able to reproduce large-scale hydroclimatic conditions. This finding is consistent with Gelaro et al. (2017), who showed that MERRA-2 effectively captures climatological means but tends to smooth local variability due to model assimilation constraints. The observed overestimation of rainfall by approximately +7 mm/month aligns with Reichle et al. (2017), who reported that MERRA-2 precipitation products often exhibit positive biases in tropical and humid regions. However, the smoothing of extreme rainfall events observed in Figure 2 is also widely documented in the literature. Studies such as Sun et al. (2018) and Tapiador et al. (2012) confirm that global reanalysis datasets systematically underestimate precipitation extremes due to spatial averaging and parameterization limitations. Despite this limitation, the seasonal cycle is well reproduced, particularly the bimodal wet season structure, which supports findings by Nkiaka et al. (2017) in Central Africa, where reanalysis products capture seasonal dynamics but struggle with local intensity variations. Overall, the results confirm that MERRA-2 is suitable for representing general precipitation patterns but less reliable for extreme event analysis.

3.5. Statistical Agreement and Error Characterization Between Observed and MERRA-2 Precipitation

The statistical evaluation highlights a moderate level of agreement between observed and MERRA-2 precipitation data, characterized by a Pearson correlation of 0.50 and an R^2 of 0.25. This indicates that while MERRA-2 captures general rainfall trends, a large portion of local variability remains unexplained. Similar conclusions were drawn by Miller et al. (2021), who reported that reanalysis datasets typically show moderate correlations with ground observations, especially in regions influenced by complex atmospheric processes such as Central Africa. The MAE of 53.14 mm and RMSE of 85.71 mm reflect substantial deviations during high rainfall periods. According to Hodson (2022), RMSE tends to emphasize large errors, particularly in hydrological datasets where extreme rainfall events dominate total variance. This explains the relatively high RMSE compared to MAE in the present study. The positive bias (+7.05 mm) further confirms a systematic overestimation of precipitation, consistent with findings from Awange et al. (2016) and Dezfuli et al. (2017), who demonstrated that satellite and reanalysis products often overestimate rainfall in African regions due to retrieval uncertainties and sparse ground validation networks. However, despite these limitations, the statistically significant relationship ($p < 0.001$) confirms that MERRA-2 remains useful for large-scale hydrological trend analysis, as also suggested by Bosilovich et al. (2017).

3.6. Comparative Analysis of Evaporation Patterns

The comparison between observed evaporation and MERRA-2 estimates reveals a strong structural inconsistency, particularly in the representation of magnitude and variability. While observed evaporation remains stable (1.70–4.10 mm/month), MERRA-2 produces unrealistic negative values and significantly lower averages. This discrepancy highlights a fundamental limitation of reanalysis-based evaporation estimation in tropical hydrological systems. This underestimation is consistent with Miralles et al. (2014), who demonstrated that evaporation estimates from global models often diverge from ground observations due to difficulties in capturing land-atmosphere interactions. Similarly, McMahon et al. (2013) emphasized that evaporation is one of the most uncertain hydrological variables in large-scale datasets, particularly in regions with limited observational constraints. The higher variability in MERRA-2 compared to station data also suggests instability in model parameterization, as confirmed by Martens et al. (2017), who showed that even advanced land-surface models struggle to accurately reproduce evapotranspiration dynamics in heterogeneous environments. The strong underestimation across all months indicates that MERRA-2 fails to capture consistent evaporative demand in the Kalamu basin, reinforcing the need for local calibration. Overall, the results indicate that MERRA-2 is not reliable for direct evaporation assessment at local scale.

3.7. Statistical Agreement and Error Characterization of Evaporation

The statistical performance of MERRA-2 for evaporation is extremely weak, as indicated by a very low coefficient of determination (R^2 = 0.019) and a weak correlation (r = 0.138). This suggests that the model explains almost none of the observed variability. Similar poor performance of reanalysis evaporation datasets has been reported by Tian et al. (2018), who found that potential evaporation products derived from reanalysis data often fail to reproduce station-level observations. The strong negative bias (−2.62 mm) further confirms systematic underestimation, which is consistent with Miralles et al. (2014), who demonstrated that global evaporation products tend to underestimate land-surface fluxes in humid regions. The presence of physically unrealistic values also reflects structural model limitations, particularly in energy balance closure and soil moisture representation. According to Hodson (2022), when RMSE and MAE values are close, errors tend to be systematic rather than random, which is exactly the case here. This reinforces the conclusion that the errors are not incidental but structural. Overall, these results confirm that MERRA-2 evaporation data should be used cautiously and primarily for qualitative rather than quantitative hydrological applications.

3.8. Hydroclimatic Variability, Hydrological Year Classification and Water Balance

The classification of hydrological years using the Z-score method reveals a climate system dominated by interannual variability rather than long-term directional change. The alternation between wet, normal, and dry years is consistent with classical hydroclimatic behavior observed in tropical regions. Similar patterns have been documented by Balme et al. (2006) in the Sahel, where rainfall variability is characterized by strong oscillations rather than persistent trends. The predominance of normal years (about 62.5%) suggests relative climatic stability at the long-term scale, while the occurrence of extreme wet and dry years highlights episodic climatic shocks. This behavior is consistent with findings from Adeyeri et al. (2020) and Okafor et al. (2017), who demonstrated that African catchments are mainly controlled by variability rather than monotonic trends. The weak long-term decline in water balance identified through Sen’s slope is not statistically significant, which aligns with Zhou et al. (2023), who emphasized that trend magnitude in hydrology is often more informative than statistical significance alone. Similarly, Kartal & Muratoglu (2026) highlighted that hydroclimatic systems may exhibit strong variability without significant trends. The calculated water deficit of 4982.05 m^3 represents the total volume of water lacking to meet the Kalamu basin demand over the studied period, mainly due to insufficient rainfall and/or high evaporation. In practical terms, this indicates that the Kalamu intake dam may not consistently supply enough water, particularly during dry seasons. To compensate for this seasonal deficit, an additional storage capacity of about 209.88 m^3 would be required. However, the current reservoir capacity is 160 m^3, which is slightly below this requirement, implying a structural storage gap. This gap reduces the system’s ability to store surplus water during wet periods for later use during dry periods, thereby increasing vulnerability to seasonal water shortages and drought stress. However, other studies indicate that while moderate deficits may occur in short-term simulations, long-term reservoir performance can sometimes remain stable if inflow variability compensates through wet-year recharge, although this depends strongly on catchment conditions and storage efficiency (Hou et al., 2022). Overall, the basin shows a stable but highly fluctuating hydroclimatic regime, requiring adaptive water management strategies to cope with alternating surplus and deficit conditions. Furthermore, the hydroclimatic results suggest that the installation of a mini-hydropower plant at the Kalamu intake dam is currently not advisable. The observed water deficit, limited storage capacity, seasonal drying of the Kalamu River, and recurrent negative water balance during the dry season indicate insufficient and unreliable water availability to sustain hydropower production without compromising the primary function of the dam, which is water supply. In addition, the absence of a significant long-term increase in precipitation and the slight decline in water balance further reduce the feasibility of hydropower development. Therefore, priority should be given to improving water storage, reservoir rehabilitation, and water resource management before considering future hydropower installation. (Hou et al., 2022; Alemu et al., 2025; Degefu et al., 2024; Mampuya et al., 2026).The methodological framework is implemented through a continuous computational workflow developed in Python within the Anaconda environment, where observed and reanalysis datasets are systematically harmonized, statistically evaluated using correlation, regression, and error metrics, and subsequently analyzed for trends and hydrological variability, ensuring a coherent, reproducible, and integrated hydroclimatic assessment, suitable for evaluating the Kalamu dam water system. The Kalamu catchment analysis highlights key management needs supported by recent studies. Reservoir storage should be increased due to observed deficits and system vulnerability (Hou et al., 2022). Adaptive management is required to address strong wet–dry variability (Alahacoon et al., 2022; Balme et al., 2006). Trend analysis should adopt multi-method approaches instead of relying solely on Mann–Kendall and Sen's slope (Zhou et al., 2023; Kartal and Muratoglu, 2026). Reanalysis datasets such as MERRA-2 require bias correction for evaporation due to known limitations (Tian et al., 2018; Martens et al., 2017; McMahon et al., 2013). Integrated monitoring improves hydrological reliability (Sun et al., 2018; Gelaro et al., 2017; Reichle et al., 2017), while advanced modelling enhances risk prediction in African basins (Adeyeri et al., 2020; Mampuya et al., 2025, 2026).

4.Conclusion

This study evaluated the hydroclimatic variability of the Kalamu catchment and its implications for water availability at the Kalamu intake dam using observed meteorological data and MERRA-2 reanalysis data for the period 1992–2023. The results demonstrated that MERRA-2 satisfactorily reproduces the general precipitation regime and seasonal rainfall patterns of the basin, although it tends to slightly overestimate precipitation and smooth extreme rainfall events. In contrast, the reanalysis product showed poor performance in representing local evaporation dynamics, with significant underestimation and weak statistical agreement with ground observations, highlighting the necessity of local calibration before operational application. The hydroclimatic analysis revealed a basin characterized primarily by strong interannual variability rather than significant long-term trends. The alternation between wet, normal, and dry years confirms the influence of climatic fluctuations on water availability within the catchment. Although the Mann–Kendall and Sen's slope analyses indicated no statistically significant trends in precipitation, evaporation, or water balance, the slight decline in water balance and increase in evaporation suggest the need for continued monitoring under changing climatic conditions. The water balance assessment identified a cumulative water deficit of 4982.05 m³ and showed that the existing reservoir storage capacity of 160 m³ is insufficient to fully compensate for seasonal shortages. The estimated additional storage requirement of approximately 209.88 m³ indicates a structural storage gap that may reduce water supply reliability during prolonged dry periods. Consequently, reservoir rehabilitation, storage expansion, and adaptive water management strategies should be prioritized to enhance the resilience of the Kalamu water supply system. Furthermore, the results indicate that the installation of a mini-hydropower plant at the Kalamu intake dam is currently not technically advisable. The combination of seasonal river drying, recurrent negative water balance during the dry season, limited reservoir capacity, and existing water deficits suggests that hydropower generation could compromise the primary function of the dam, namely domestic water supply. Therefore, future investments should focus first on improving water storage infrastructure, hydrological monitoring, and catchment management before considering hydropower development. Overall, this study contributes to the understanding of hydroclimatic variability in the Kalamu catchment and provides a scientific basis for sustainable water resources management. The findings support evidence-based decision-making for reservoir operation, climate adaptation planning, and long-term water security in Boma and similar tropical catchments facing increasing hydroclimatic uncertainty.

Data Availability

The data used to support the findings of this study are available from the corresponding author upon request.

Conflicts of Interest

The authors declare that they have no conflicts of interest regarding the publication of this paper.

Acknowledgment

The authors gratefully acknowledge the Boma Meteorological Station for providing observational climate data and NASA GMAO for access to MERRA-2 reanalysis datasets.

References

Adeyeri, O. E., Laux, P., Lawin, A. E., Ige, S. O., & Kunstmann, H. (2020). Analysis of hydrometeorological variables in the Komadugu-Yobe transboundary basin, West Africa. *Journal of Water and Climate Change*, 11(4), 1339–1354.

Alahacoon, N., Edirisinghe, M., Simwanda, M., Perera, E., Nyirenda, V. R., & Ranagalage, M. (2022). Rainfall variability and trends across the African continent using TAMSAT data (1983–2020): Towards resilience and adaptation to climate change. *Remote Sensing*, 14(1), 96.

Alemu, M. M., Zaitchick, B. F., Enku, T., Worqlul, A. W., Yimer, E. A., & van Griensven, A. (2025). Hydroclimatic dynamics assessment: Trend analysis and change detection for improved drought monitoring in the upper Blue Nile basin. *Water and Climate Change Review*, 16(8), 2519–2537.

Awange, J. L., Mpelasoka, F., & Goncalves, R. M. (2016). When every drop counts: Analysis of droughts in Brazil for the 1901-2013 period. *Science of the Total Environment*, 566, 1472–1488.

Balme, M., Lebel, T., & Amani, A. (2006). Dry and wet years in the Sahel: Quo vadimus? *Hydrological Sciences Journal*, 51(2), 254–271.

Bosilovich, M. G., Robertson, F. R., Takacs, L., Molod, A., & Mocko, D. (2017). Atmospheric water balance and variability in the MERRA-2 reanalysis. *Journal of Climate*, 30(4), 1177–1196.

Degefu, S. B., Alamirew, T., & Demessie, S. F. (2024). Analysis of trends and variability of hydroclimatic variables in the Didessa sub-basin: Implications for the upper Blue Nile (Abbay) basin, Ethiopia. *Heliyon*, 10(23), e40534.

Dezfuli, A. K., Ichoku, C. M., Huffman, G. J., Mohr, K. I., Selker, J. S., van de Giesen, N., ... & Annor, F. O. (2017). Validation of IMERG rainfall in Africa. *Journal of Hydrometeorology*, 18(10), 2817–2825.

Fernández-Pato, J., Caviedes-Voullième, D., & García-Navarro, P. (2016). Simulation of rainfall/runoff with complete 2D equations in shallow water: Sensitivity analysis and calibration of infiltration parameters. *Journal of Hydrology*, 536, 496–510.

Gelaro, R., McCarty, W., Suárez, M. J., Todling, R., Molod, A., Takacs, L., ... & Zhao, B. (2017). The modern-era retrospective analysis for research and applications, version 2 (MERRA-2). *Journal of Climate*, 30(14), 5419–5454.

Hodson, T. O. (2022). Root mean square error (RMSE) or mean absolute error (MAE): When to use them and when not to. *Discussions on the Development of Geoscience Models*, 2022, 1–10.

Hou, J., Van Dijk, A. I., Beck, H. E., Renzullo, L. J., & Wada, Y. (2022). Water storage dynamics in remote reservoirs (1984–2015) and the influence of global climate variability and management. *Hydrology and Earth System Sciences*, 26(14), 3785–3803.

Kartal, V., & Muratoglu, A. (2026). Une compréhension des tendances hydrométéorologiques: Une évaluation multi-méthodes des tendances. *Water Resources Management*, 40, 199.

Mampuya Nzita, A., Umba-di-Mbudi, N. Z., Makanzu Imwangana, F., & Dituba Ngoma, G. (2025). Performance comparison of PSO and GA algorithms in predictive modeling of flood-related deaths in Boma. *Journal of Hydraulic and Water Engineering*, 2(2), 125–144.

Mampuya, A. N., N'zau, C. U. D. M., Makanzu, F. I., & Dituba, G. N. (2026a). Flood modeling in Boma: Relationships between water level of the Congo River, flow of the Kalamu River and social risks. *Revue Congolaise des Sciences et Technologies*, 5(1), 250–258.

Mampuya, A. N., N'zau, C. U. D. M., Ntumba, J. K., & Dituba, G. N. (2026b). Use of artificial intelligence for modeling the flows of the Kalamu River and the Congo River in Boma for energy security. *Revue Congolaise des Sciences et Technologies*, 5(1), 181–191.

Martens, B., Miralles, D. G., Lievens, H., Van der Schalie, R., De Jeu, R. A., Fernández-Prieto, D., ... & Verhoest, N. E. (2017). GLEAM v3: Satellite-based land evaporation and root zone soil moisture. *Geoscientific Model Development*, 10(5), 1903–1925.

McMahon, T. A., Peel, M. C., Lowe, L., Srikanthan, R., & McVicar, T. R. (2013). Estimation of actual, potential, reference evaporation of crops and patches from standard meteorological data: A pragmatic synthesis. *Hydrology and Earth System Sciences*, 17(4), 1331–1363.

Miller, D. E., Wang, Z., Li, B., Harnos, D. S., & Ford, T. (2021). Skillful prediction of subseasonal extreme hot days in the United States and standardized precipitation index in boreal summer. *Journal of Climate*, 34(14), 5887–5898.

Miralles, D. G., Van Den Berg, M. J., Gash, J. H., Parinussa, R. M., De Jeu, R. A., Beck, H. E., ... & Johannes Dolman, A. (2014). El Niño–La Niña cycle and recent trends in continental evaporation. *Nature Climate Change*, 4(2), 122–126.

Nkiaka, E., Nawaz, N. R., & Lovett, J. C. (2017). Evaluation of global precipitation reanalysis datasets with rain gauge measurements in the Soudano-Sahel region: Case study of the Logone watershed, Lake Chad basin. *Meteorological Applications*, 24(1), 9–18.

Okafor, G., Jimoh, O., & Larbi, K. (2017). Detecting changes in hydro-climatic variables during the last four decades (1975-2014) on downstream Kaduna River catchment, Nigeria. *Atmospheric and Climate Sciences*, 7, 161–175.

Reichle, R. H., Liu, Q., Koster, R. D., Draper, C. S., Mahanama, S. P., & Partyka, G. S. (2017). Land surface precipitation in MERRA-2. *Journal of Climate*, 30(5), 1643–1664.

Rienecker, M. M., Suarez, M. J., Gelaro, R., Todling, R., Bacmeister, J., Liu, E., ... & Woollen, J. (2011). MERRA: NASA's retrospective analysis in the modern era for research and applications. *Journal of Climate*, 24(14), 3624–3648.

Seager, R., Osborn, T. J., Kushnir, Y., Simpson, I. R., Nakamura, J., & Liu, H. (2019). Climatic variability and evolution of Mediterranean-type climates. *Journal of Climate*, 32(10), 2887–2915.

Sun, Q., Miao, C., Duan, Q., Ashouri, H., Sorooshian, S., & Hsu, K. L. (2018). A review of global precipitation datasets: Data sources, estimation and intercomparisons. *Reviews of Geophysics*, 56(1), 79–107.

Tapiador, F. J., Turk, F. J., Petersen, W., Hou, A. Y., García-Ortega, E., Machado, L. A., ... & De Castro, M. (2012). Global precipitation measurement: Methods, datasets and applications. *Atmospheric Research*, 104, 70–97.

Tian, Y., Zhang, K., Xu, Y. P., Gao, X., & Wang, J. (2018). Evaluation of potential evapotranspiration based on CMADS reanalysis dataset over China. *Water*, 10(9), 1126.

Wang, Y., Gueye, M., Greybush, S. J., Greatrex, H., Whalen, A. J., Ssentongo, P., ... & Schiff, S. J. (2023). Verification of operational forecasts of the numerical weather forecasting model of precipitation using satellite estimates of precipitation in Africa. *Weather Applications*, 30(1), e2112.

Xiong, J., Xu, L., Chandanpurkar, H. A., Famiglietti, J. S., Zhang, C., Ghiggi, G., ... & Vishwakarma, B. D. (2023). ET-WB: Water balance-based estimates of terrestrial evaporation over global lands and major global basins. *Earth System Science Data*, 15(10), 4571–4597.

Zakwan, M., & Ahmad, Z. (2021). Trend analysis of hydrological parameters of River Ganga. *Arabian Journal of Geosciences*, 14(3), 163.

Zhou, J., Deitch, M. J., Grunwald, S., & Screaton, E. (2023). Don't the Mann-Kendall test and Theil-Sen slope provide information on the significance and magnitude of trends in hydrology? *Hydrological Sciences Journal*, 68(9), 1241–1249.